Design and Construction of an Isolated Matrix Converter for DC networks

Rui Pedro Mac-Mahon Fartaria Moreira

Department of Electrical and Computer Engineering

Instituto Superior Técnico - Technical University of Lisbon, Portugal

Email: ruimoreira@tecnico.ulisboa.pt

***Abstract* — The evolution of the technology in the area of power electronics has been quite noticeable in the past years, namely in the development of new semiconductors, such as JFET semiconductors, that are able to operate in systems needing very high switching frequencies (hundreds of kHz).**

It is proposed to design and construct a prototype of a modified matrix converter which encompasses the sizing, assembly and laboratory tests, with the aim of being coupled to a high frequency transformer and a rectification system on primary and secondary side to obtain a low capacitance AC-DC converter for use in future tertiary DC networks.

The circuit of rectification and acquisition of currents and voltage was mounted on printed circuit boards and for that, it was necessary to carry out the sizing of both printed circuit boards, design and drawing, assembly of components and validation through tests. Starting from the general scheme, the matrix converter is being decomposed into its constituent parts, thus allowing phased realization of the description and dimensioning of each of them, namely; the power circuit and its protections; the control device, which through the galvanic isolation allows the digital signals generated by a microprocessor to be transmitted to the power semiconductors; the voltage and current acquisition circuit whose function is to provide the Digital Signal Processor (DSP) with images of both input and output voltages and currents.

***Index Terms* — Matrix Converter; Power Semiconductors; Matrix Converter; Rectification; Power Modules, Data acquisition**

I. INTRODUCTION

In the last years there is a big motivation to electrical energy generation in a decentralized way, using clean energy resources, like solar and wind. The local generation and consumption would avoid transport losses, improving the affordability of electrical networks. However, the inter-connection of sources, like DC (solar) and AC (wind), with different voltage levels and waveforms, implies their adaptation through electronic power converters and their use in micro-grids has to follow well defined characteristics.

Main electric networks will continue to use AC voltages for compatibility reasons and easy voltage level transformation. However, nowadays most electric loads need DC power obtained via AC-DC switching converter, between the AC input voltage
230V and the DC output voltage from 5V to 400V. Therefore, most actual loads such as lighting systems [1], small appliances and mobile devices could advantageously be supplied from a common DC network, eliminating the need of the embedded AC-DC converter and sparing its losses.

With the recent progress in the semiconductor technologies a single high efficiency central AC-DC converter could be advantageous in eliminating several less reliable and less efficient AC-DC embedded converters. Even if the DC voltage needs to be customized, a DC-DC converter is simpler and presents higher efficiency than an AC- DC converter.

Considering also the High Voltage Direct Current (HVDC) technology DC buses are currently an alternative to AC grids, with better use of resources, both in transmission, distribution and in the final consumer place. These advantages will be emphasized by the integration of electric vehicles, as they require a large amount power to handle the fast charging of batteries. The fast charging process may benefit from the DC grid due to the simplicity and efficiency of DC-DC converters compared to the typical AC-DC [2]. Moreover, in DC networks there is no reactive power compensation, no need to synchronize generators for the network frequency, no skin effect and easier power failure mitigation when combined with energy storage systems. On the other hand, DC networks are not directly connectable to electric machines, such as transformers and motors demanding the use of switching converters (at least diode bridge rectifiers for doubly fed induction motors driven with
3 phase inverters). Additionally, it is necessary to adapt the handling equipment including equipment and people

protections, while needing an efficient isolated AC- DC converter to link with the mains network [3].

In this framework, the research question is how to implement the concept of AC- DC power converters with galvanic insulation, but without the use of intermediate electrolytic capacitor DC buses, to provide energy to a DC micro-grid.

This dissertation propose the use of a single-phase AC-DC power converter, using high frequency transformer isolation, to interconnect the AC power distribution grid network at unity power factor and to supply a DC micro-grid for residential or commercial complex use, with the target of reducing losses, cost and footprint, ensuring required quality parameters for suppliers and consumers.

A. *Single-Phase Matrix Converter*

The single-phase matrix converter consists of four bidirectional switches fully controlled [4], allowing the interconnection of two single-phase systems, one with characteristics of voltage source and another with characteristics of current source (Figure 1).

Assuming that the bidirectional semiconductor switches have an ideal behaviour (zero voltage when they are ON, zero leakage current when they are OFF and nearly zero switching time), and each of the switches can be represented mathematically by a variable S_{kj} which can take the value of "1" if the switch is closed (ON) and the value of "0" if the switch is open (OFF).

One can represent the state of the converter in a 2x2 matrix (1).

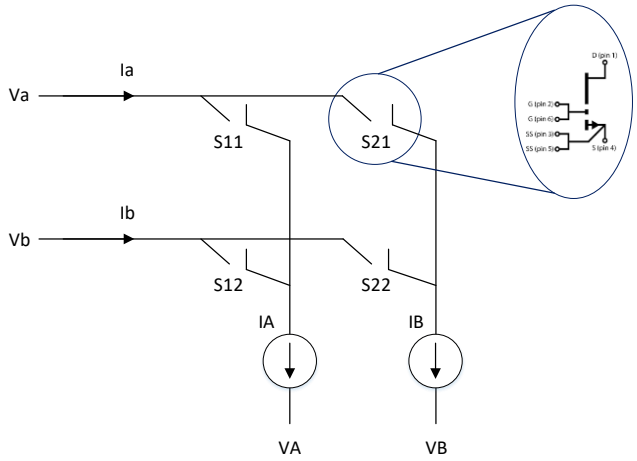

Figure 1 - Single-Phase Matrix Converter

We must take into account compliance with the topological constraints, implying that in each time step, each phase output is only connected to one and only one input phase.

$$\boldsymbol{S} = \begin{bmatrix} S_{11} & S_{12} \\ S_{21} & S_{22} \end{bmatrix} \quad (1)$$

In Table I are described four possible states, with the respective correlations between the electrical variable combinations.

Table I – Possible switch combinations for a Single-Phase Converter

Name	*States*		*S11*	*S12*	*S21*	*S22*	*Vo*
S_{10}	$X_A = 1$	$X_B = 0$	ON	OFF	OFF	ON	$+V_i$
S_{00}	$X_A = 0$	$X_B = 0$	OFF	OFF	ON	ON	0
S_{11}	$X_A = 1$	$X_B = 1$	ON	ON	OFF	OFF	0
S_{01}	$X_A = 0$	$X_B = 1$	OFF	ON	ON	OFF	$-V_i$

B. *High frequency transformer*

Today, power electronics are increasingly present in power systems, directed at transforming and converting electricity energy through semiconductors. It is in this area that the High Frequency transformer is applied, typically in conjunction with switched sources, converters, solid state transformers, among others.

Figure 2 represents the positioning of the high frequency transformer in the converter voltage source [5]. In most situations, transformers, only works as galvanic isolation, for the protection and safety of equipment and people. The regulation of tensions is made by the power electronics.

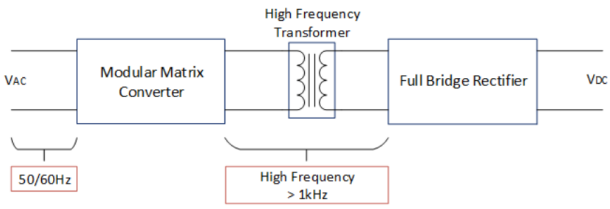

Figure 2 – Simplified scheme oh high frequency transformer

II. GLOBAL OVERVIEW OF THE MATRIX CONVERTER

The global schematic of the matrix converter is shown on Figure3. In this chapter it will be performed the description of all its parts, on the next two the sizing of the components will

be performed, one chapter will be devoted to the matrix converter and another one to the voltages and currents acquisition circuit with voltage source characteristics and the output system with characteristics of current source. These converters allow direct AC-DC conversion, without an intermediate but with a high efficiency guaranty.

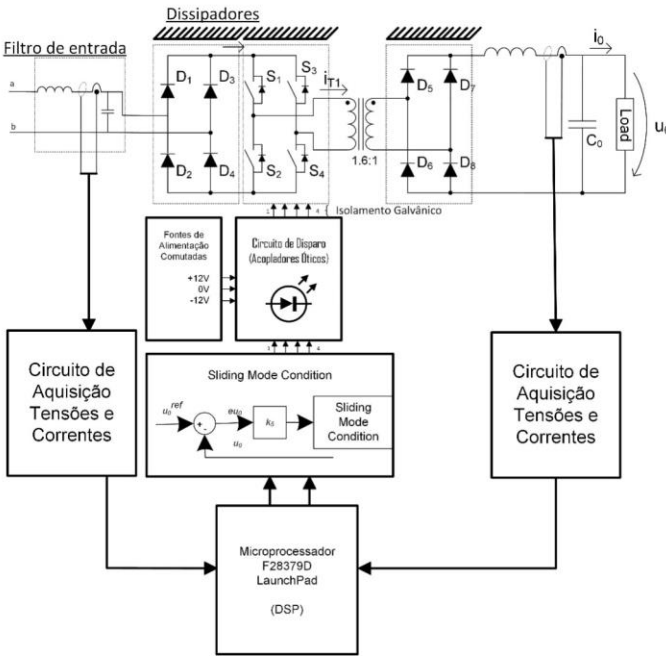

Figure 3– Matrix converter global schematic

Figure 3 is composed of three main parts, namely, the power circuit, the control and command circuit and the voltage and current capture circuit. These parts can be subdivided into:

A. Power circuit:

1) Power Modules (JFET Transistors);
2) Heat Sinks;
3) Rectifier Bridges.

B. Command and drive circuit:

1) Command circuit:

- *Output voltage control using sliding mode control;*

2) Drive circuit (Optocouplers);
3) Switching power supplies.

C. Voltage and current acquisition circuit.

III. MATRIX CONVERTER COMPONENTS SIZING

After the description of all the elements that compose the modified matrix converter and de voltages and currents acquisition circuit, in this chapter and the next the sizing of them will be performed.

It is important to start first by defining the operation regimes of the matrix converter regarding power and current.

With the matrix converter working with a maximum power of 1 kVA, the currents are obtained in primary side with (2).

$$S = V_{Grid} * I_{Grid} \quad (2)$$

To calculate the current to be supplied by the DC side (3), disregarding the losses in the circuit and considering the same power, an output voltage of 48V is intended. Thus, it results, considering almost unitary power factor:

$$U_{DC} * I_{Out} = V_{Grid} * I_{Grid} \quad (3)$$

The current calculation for the primary (2) and secondary side (3) side currents are crucial for the calculation of the printed circuit lane width, the sizing of the heatsinks and the calculation of the circuit losses.

A. Power Circuit

For the desired operating state, JFET GS66516B, manufactured by GaN Systems Inc have been chosen, because those are the semiconductors that better suit to the frequency of commutation desired. This power semiconductor will be chosen because it has properties to operate comfortably at 1kVA power.

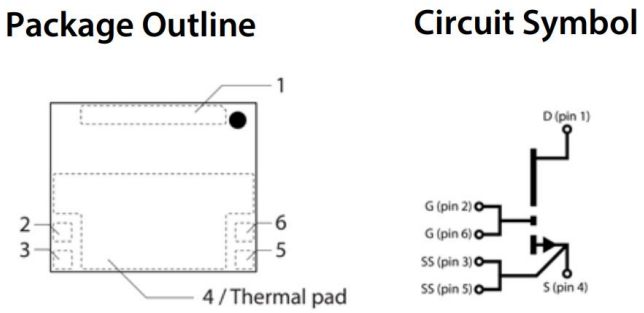

Figure 4 - JFET GS66516T Symbol and Footprint.

B. Full Wave Rectifier

For the construction of both rectifier bridge plates, primary and secondary currents, diode voltages and operating frequencies on the primary and secondary side were considered.

1) Primary side

For the primary side, the semiconductor chosen for the rectifier board construction was the Vishay VS-80APS12-M3 diode. This diode has a low cost and a low voltage between the anode and cathode when it is in commutation. It has an $I_{F(av)} = 80A$ and a $V_{RRM} = 1200V$.

2) Secondary side

On the secondary side, for the rectifying bridge it has to be taken into account that an alternating voltage with a frequency of 20kHz is rectified. This required the use of Schottky diodes. The use of fast switching diodes is essential at high frequencies to minimize switching losses. These diodes provide the ideal conditions for high frequency operation, having switching times of I_{rr} near μ_A. The diodes chosen for the rectifier bridge are C5D50065D manufactured by Cree Inc.

IV. SNUBBERS

The application at high frequencies of inverse voltage values causes the appearance of inverse currents, which can reach significant values.

Schottky effect diodes do not have significant inverse recovery currents, but being almost capacitive causes high frequency oscillations [6]. To reduce them and prevent a substantial increase in the (dV/dt) variation at the terminals of each rectifier bridge diode, a protective $R_S C_S$ snubber was used at the input terminals to dampen voltage fluctuations and limit the rate of change of direct voltage.

The purpose of this snubber is to protect against over voltages that may occur between the anode and cathode when passing through the driving and also when they pass to the cut.

Figure 5 shows how the $R_S C_S$ snubber was installed on each of the rectifier bridges.

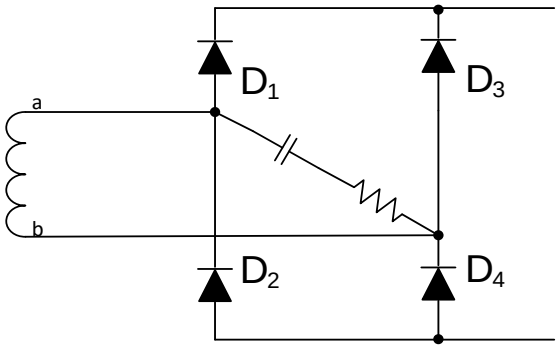

Figure 5 – Illustration of mounting of the snubbers on each rectifier bridge.

The damper capacitor sizing (C_S) can be calculated, just as the magnetic energy stored in the coil (L_S) is transferred to a hypothetical C_s'. The equality of the energies in the capacitor C_S 'and the coil L_S considering that the diode cutoff is made with the reverse recovery current (I_{RR}), is given by (4):

$$\frac{1}{2}U^2 C_s' = \frac{1}{2}L_s {I_{rr}}^2 \quad (4)$$

In general, the value of I_{RR} of the direct current in the diode and its variation in time is usually imposed by the coil L_S. However, C_s' can be calculated from the maximum diode reserve recovery charge Q_{rr} and the diode snapiness factor Λ. Expressing C_s'' as a function of Q_{rr}. (5), we have:

$$C_s' \approx \frac{Q_{rr}}{U} * \frac{2\Lambda}{(2-\Lambda)} \quad (5)$$

Since in the secondary the output voltage has only a continuous component with a voltage in the order of 48V, the resistance of the snubber R_S has been dimensioned to guarantee a damping factor (ξ) in the circuit such that an overvoltage of the voltage v_{AK} in the order of $\approx$ 50% is obtained. For this, it was considered a $\xi \approx 0{,}4$ and $C_S \approx 2\, C_s'$. The resistance value can be given by (6):

$$R_S = 2\,\xi \sqrt{\frac{L_S}{C_S}} \quad (6)$$

Table III shows the summary of the parameters of the diode's overvoltage protection dimension.

Table III - Summary of the parameters of diode overvoltage protections.

Parameters of snubbers	
C_S	R_S
$2nF$	25.3Ω

V. POWER LOSSES

The power loss in the matrix converter and the two rectifying bridges consist on two components, namely, the losses resulting from the conduction and the losses resulting from the switching of the power semiconductors. Both losses are calculated based on the characteristics provided by the manufacturer. However, for the primary side rectifier bridge diodes it is necessary to do some laboratory tests due to the scarcity of information provided by the manufacturer in order

to calculate the switching losses. Figure 6 shows the current and voltage at the terminals of each diode of the circuit, the output voltage of the modified matrix converter and the circulating currents in the power semiconductors.

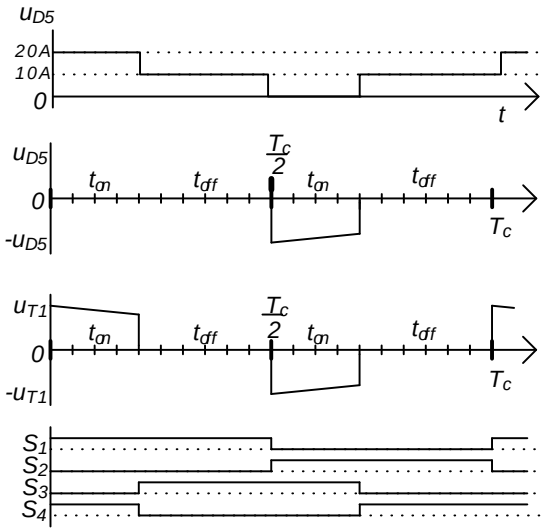

Figure 6 - Current and Voltage Diagram

A. Power losses Bridge Rectifier

To calculate the diode losses that are installed on both rectifier bridges, the switching losses are calculated by equation (7) and the conduction losses are calculated by (8), where i_{AKDC}represents the average value of the terminals current diode and $I_{AK_{RMS}}$the effective value of the diode current at the terminals. Respectively:

$$P_C = V_d i_{AKDC} + r_D I_{AK_{RMS}}^2 \tag{7}$$

$$P_{COM} = \frac{UI_{RR}(t_{rr} - t_s)}{T} = \frac{UQ_{rr}}{T}\frac{(1-\Lambda)}{(1-\Lambda/2)} \tag{8}$$

For the calculation of conduction losses, a period $T = 20ms$ was considered for the primary side rectifier bridge and a $T = 50\mu s$ for the Matrix Converter and secondary side rectifier bridge conduction losses.

B. Power losses modified Matrix Converter

In addition to the rectifying bridges, it is necessary to calculate the losses of the modified matrix converter. For the calculation of the modified matrix converter losses, the conduction (9) and commutation (10) losses are given by:

$$P_C = r_{Dson} * \left(I_{rede} * \sqrt{\delta}\right)^2 \tag{9}$$

$$P_{COM} = V_{rede} * I_{rede} * \frac{t_{off} + t_{on}}{2} * f_s \tag{10}$$

VI. Acquisition of Voltages and Currents

A. Voltage Acquisition Circuit

Its construction required its correct dimensioning to guarantee an input voltage on the microcontroller within the ideal parameters, thus ensuring its proper functioning.

The voltage acquisition circuit is based on transforming input voltages into signals of acceptable levels so that they can be read by the microcontroller, 230V effective voltages on signals of approximately $3V_{pp}$. This microcontroller does not accept negative voltages, and the addition of a continuous voltage U_{ref} is required to prevent any damage to the microcontroller. It is referenced to a DC voltage of $1.5V$ enough that the microcontroller can read a voltage in the range $[0V \quad 3V]$.

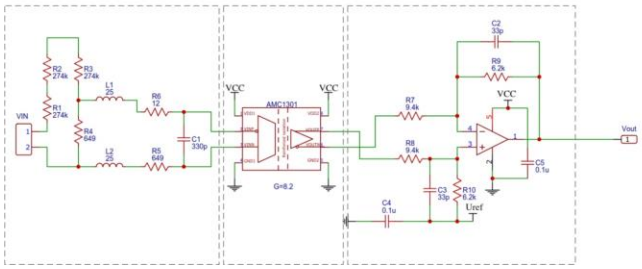

Figure 7 - Voltage Acquisition Circuit

The voltage acquisition circuit is divided into three parts, namely, a voltage divider, a reinforced isolated amplifier and finally a voltage subtractor amplifier.

B. Current Acquisition Circuit

The purpose of this circuit is to provide to the microcontroller with the image of the current, which will be required at four points of the modified matrix converter, represented in Figure 3. For the semiconductor switching process, it is essential to know the signal of the currents for correct operation. If the current has the direction of the source to the load the switching process takes place in one way, if the direction is from the load to the source the switching will be different as previously studied. For the design of the current

acquisition circuit, the methodology is identical to that of the voltage acquisition circuit, however it is necessary to insert and remove some components to obtain an image within the allowable parameters to be read by the microcontroller. Figure 8 shows the current acquisition circuit.

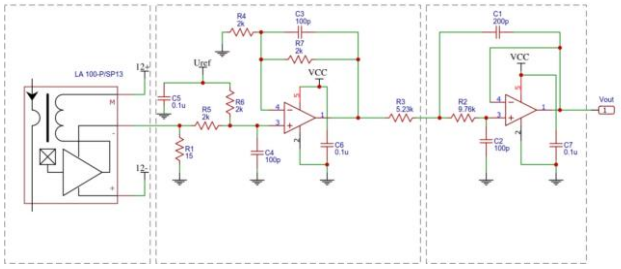

Figure 8 - Current Acquisition Circuit

This circuit is composed by three blocks, namely, a current transducer, a buffer with a built-in shifter, adding a DC voltage and finally a 2nd order low-pass filter.

VII. PRINTED CIRCUIT BOARD DESIGN

The design of the PCB layout was achieved by applying the standards compiled on the IPC, namely both the IPC-2221 and IPC-9592, the first one has the rules of thumb for printed board design and the second is applied to power conversion devices.

From these documents wore obtained the spacing between tracks according to the voltage, in this case was considered the phase-to-neutral 230 $V_{RMS,}$ and the tracks width according to the maximum current.

Figure 9 presents the final layout of the primary and secondary side bridges, following the standards described above.

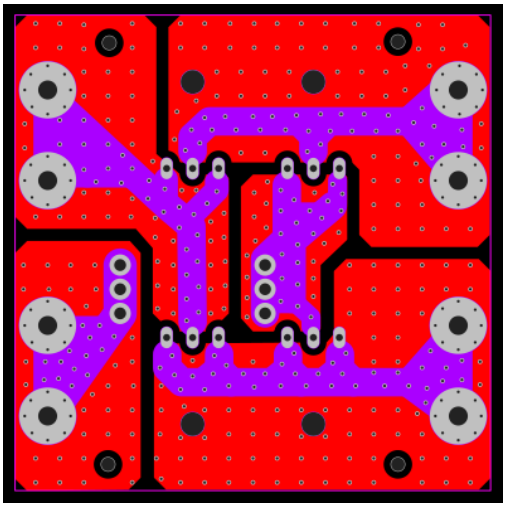

Figure 9– Full Bridge Rectifier layout

VIII. RESULTS

It was intended to compare the theoretical results with the experimental results to confirm the correct functioning of all components.

In order to ensure that all connections were made correctly, we started by ensuring the validation of each component part of the Matrix Converter separately and after verifying their correct operation, the final assembly of the Matrix Converter was performed and then the final test was performed.

In a first approach, the design of semiconductor overvoltage protections will be implemented to verify that the theoretical calculations correspond to the intended ones.
Then the voltage and current acquisition board will be tested to ensure that the signals from the DSP are within the desired values, adjusting if necessary, some constituent parts of this board.

A. Practical test of over voltage protection

Figure 10 presents the test performed at the voltage v_{Ak} of the secondary rectifier board diodes, when they go from direct to reverse bias without overvoltage protection. It can be seen that at time t_{rr}, the voltage v_{Ak} is almost twice the operating voltage, which increases switching losses and can lead to the destruction of semiconductors. The circuit was fed by applying a voltage set on the autotransformer to $V_{rms} = 135V$ over a resistive load of $50\ \Omega$.

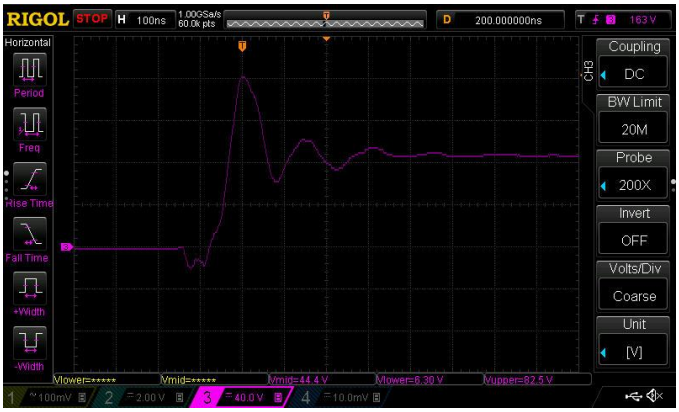

Figure 10 – Voltage v_{Ak} to diode terminals without snubbers

After adding the R_SC_S snubber, Figure 11 shows again the test performed at the voltage v_{Ak} of the secondary side rectifier plate diodes, when they go from direct to reverse bias. It can be seen that at time $t_{rr}$the voltage v_{Ak}has a very slight increase over the voltage V_{rms}, which substantially decreases the overvoltages, concluding that the snubber is doing its intended purpose.

Figure 11 – Voltage v_{Ak} to diode terminals with snubbers

B. Experimental Test of Voltage and Current Acquisition circuit

1) Voltage Acquisition circuit

For the analysis of the voltage acquisition circuit, during the experimental test, an input function generator with a voltage of 7.5V was used. Through the output voltage, with the frequency increase, the objective was to study the phase offset and amplitude of the output voltage.

Figure 12 shows the frequency response during the experimental tests.

To test the voltage and current acquisition plate a signal generator was used. The board was powered at 0V and ± 12 V by applying an external current source. It was intended to obtain the output voltage and current waveforms and the frequency response of both circuits.

For the test of the actual gain of the voltage acquisition circuit, a variation of alternating voltages with a step of 20V in the range [-360 360] V was inserted at the input. Figure 12 shows the results obtained during the experimental test, in which a line was drawn over the points read at the circuit exit. The slope of the line represents the total gain of the circuit, where in the ordinates the input voltage is represented and in the coordinates the output voltage.

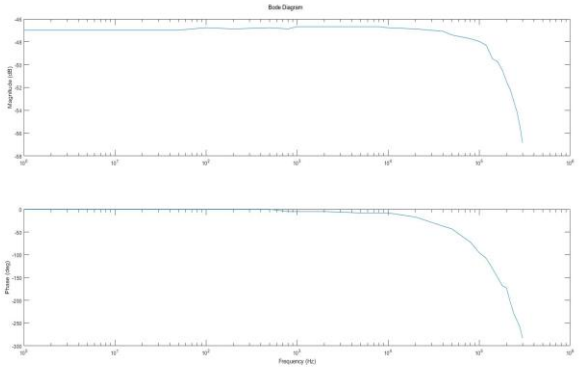

Figure 12 - Bode diagram of the voltage acquisition circuit

2) Current Acquisition circuit

For the experimental test an input function generator with a maximum voltage of 600mV at the 15Ω resistance, to generate the desired signal. The LEM's for this particular test were not used to avoid the use of high voltages.

Figure 4.4.5 shows the frequency response during the experimental tests. In both cases, it is possible to verify that the obtained values are quite identical to the theoretical results, and it can be concluded that the current acquisition circuit is in good working condition.

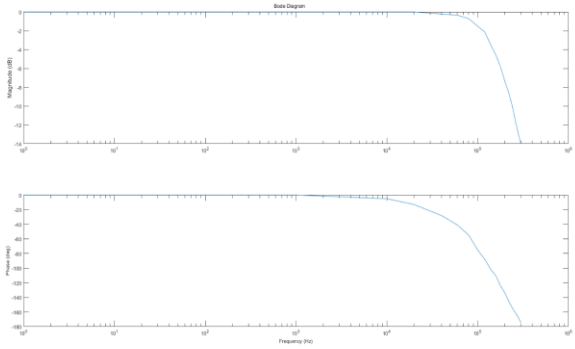

Figure 12 - Bode diagram of the current acquisition circuit

IX. Conclusions and Future Work

In this work aimed the objective to build and test in the laboratory a single phase modified matrix converter capable of supplying power up to 1kW. In the construction process it was necessary to design several constituent parts, namely the voltage and current acquisition circuits necessary for the power semiconductor switching process of the modified matrix converter. The rectifying bridges were also dimensioned and built, where it was necessary to install overvoltage snubbers in the power semiconductors, as well as the heatsink where the semiconductors were housed.

During the development of this project, several concerns arose, such as the high current on the secondary side of the Matrix Converter, where it was necessary to study the semiconductors to be used to ensure correct operation.

From the results analysis, it can be concluded that the constituent parts of the modified matrix converter have a correct functioning.

The work carried out in this master thesis will serve for future design methodologies and the construction of new matrix converters, with the perspective of proposing applications for these converters.

With the work developed here, it is facilitated the development of matrix converters with suitable characteristics to be able to be connected to several devices.

REFERENCES

[1] R. Chauhan, B. Rajpurohit, R. Hebner, S. Singh, and F. Gonzalez-Longatt, “Voltage Standardization of DC Distribution System for Residential Buildings”, Journal of Clean Energy Technologies, Vol. 4, No. 3, May 2016

[2] Public Overview of the Emerge Alliance Data/Telecom Center Standard “Emerge Alliance Advances DC Power to the Desktop”, EMerge Alliance, San Ramon, CA, USA, 2012

[3] G. Priyadharshini, N. R. Nandhini, S. Shunmugapriya and R. Ramaprabha, "Design and simulation of smart sockets for domestic DC distribution," 2017 International Conference on Power and Embedded Drive Control (ICPEDC), Chennai, 2017, pp. 426-429.

[4] Zuckerberger, A.; Weinstock, D.; Alexandrovitz, A.; “Single-phase Matrix Converter”, IEE Proceedings Electronic Power Applications, Vol.144, No 4, pp. 235-240, July 1997

[5] Pedro, F: “Transformador Eletrónico de Potência para Aplicações em Sistemas de Energia”. MSc Thesis, Instituto Superior Técnico, Universidade Técnica de Lisboa, 2014.

[6] J. F. Silva, “Electrónica Industrial Semicondutores e Conversores de Potência, série Manuais Universitários,” Lisboa, Fundação Calouste Gulbenkian, 2013,